JOURNAL OF GEOPHYSICAL RESEARCH, VOL. 106, NO. D22, PAGES 28,259–28,274, NOVEMBER 27, 2001

Predicted hygroscopic growth of sea salt aerosol

Yi Ming

Department of Civil and Environmental Engineering, Princeton University, Princeton, New Jersey

Lynn M. Russell

Department of Chemical Engineering, Princeton University, Princeton, New Jersey

Abstract. Organic species in sea salt particles can significantly reduce hygroscopic growth in subsaturated conditions, an important uncertainty in the radiative effect of aerosol particles on the atmosphere. This hygroscopic behavior is predicted with a numerical model of the the organic-water, electrolyte-water, and organic-electrolyte interactions in complex mixtures of organic species and inorganic ions. The results show a 15% decrease in hygroscopic growth above 75% relative humidity for particles that include as little as 30% organic mass. Organic compositions of 50% organic mass reduce hygroscopic growth by 25%. This prediction relies on particle chemical composition estimated from measurements of insoluble organic species in marine-derived particles and of soluble organic species measured in seawater. Twenty insoluble and four soluble organic species are used to represent the behavior of sea salt organic composition. The hygroscopic growth is strongly sensitive to the organic fraction that is soluble or slightly soluble, although variations among different soluble or insoluble species are small above the sodium chloride deliquescence point. Interactions between organic and electrolyte species depend primarily on the "salting out" behavior of NaCl with alkanes, carboxylic acids, and alcohols, although interactions with other inorganic ions in sea salt were estimated to cause small changes in the hygroscopic growth. The predicted growth factors for sea salt with $< 30\%$ organic species are consistent with growth factors measured for ambient marine-derived particles by another group [*Berg et al.,* 1998; *Swietlicki et al.,* 2000; *Zhou et al.,* 2001]. This coincidence suggests that the less-hygroscopic particles could indicate the presence of marine organic compounds, although multiple combinations of inorganic and anthropogenic organic species would also satisfy the measured behavior.

1. Introduction

Sea salt aerosol particles in the marine boundary layer (MBL) are produced from the evaporation of sea spray [*Blanchard*, 1983]. Surface active organic materials in seawater can contribute to the aerosol phase as part of the bubble-bursting process [*Hoffman and Duce*, 1976]. The resulting internally mixed aerosol of salt ions and organic species form a significant fraction of the aerosol particles in the marine boundary layer [*Blanchard*, 1964]. These particles contribute to atmospheric radiative transfer indirectly by serving as cloud condensation nuclei and directly by scattering light in subsaturated conditions [*Seinfeld and Pandis*, 1997; *Haywood et al.*, 1999].

The optical properties of aerosol particles are greatly influenced by their chemical composition as well as their size [*Tang et al.*, 1997]. Organic components will affect the particle refractive index and the size that a particle becomes by taking up water from the vapor phase in humid conditions. Water-soluble components of aerosol are more likely to take up water because the resulting aqueous solution will have a reduced water activity. *Saxena and Hildemann* [1996] found that multifunctional organic compounds that have more than one polar functional group, such as both an alcohol group (-OH) and an acid group (-COOH), in the same carbon chain were likely to absorb water. Since both salts and organic components can be internally mixed in sea salt aerosol, particle hygroscopicity is determined by complex solutions of electrolytes, organic species, and water. The variety of chemical structures of organic compounds found in aerosol leads to a wide range of physical and chemical properties. This complexity poses difficulties for identifying particle components.

Empirical models of inorganic aerosol compare well with extensive empirical data [*Zhang et al*, 2000]. However, descriptions of the behavior of mixtures of the

Paper number 2001JD000454.
0148-0227/01/2001JD000454$09.00

Table 1. Direct Measurements of Sea Salt Particle Chemical Composition

Compound Type	Location 1: Island of Crete[a]		Location 2: Marshall Islands[b]	
	Carbon Number Range	Total Concentration, ng m^{-3}	Carbon Number Range	Total Concentration, ng m^{-3}
Aliphatic alkanes	15–40	5.09–35.24	21–36	0.020–0.16
PAHs		0.07-2.0		
n-Alkanals	15–30	0.9–16.85		
Alkanones	10–31	0.4–5.12		
n-Alkanols	12–30	2.74–94.50	13–20	0.060–0.255
Fatty acids and their salts	8–32	24.26–124.30	13–32	0.163–5.051

[a]From *Gogou et al. [1998].*
[b]From *Duce et al. [1983].*

myriad of organic compounds present in aerosol are still in the early stage [*Saxena and Hildemann*, 1997]. In addition to needing a model of the solution thermodynamics, an accurate description of the phase equilibrium of electrolyte-organic solutions requires knowing the composition of sea salt particles. Since only some sea salt components have been identified to date, we use an estimated sea salt composition that incorporates all of the known organic and inorganic species in particles of different sizes. This model serves as a reference to study the sensitivity of hygroscopic growth to uncertainties in composition as well as in organic-water and organic-electrolyte interactions that control equilibrium. The predicted hygroscopic growth also allows us to compare the behavior of the model composition to field measurements of ambient aerosol.

2. Chemical Composition of Sea Salt Aerosol

Sodium chloride (NaCl) is the major inorganic component of sea salt particles that are produced at the ocean surface. Both dissolved and particulate organic components in seawater are added to atmospheric aerosol by these same ocean processes. Typically only 10% or less of the total organic particle mass has been resolved into individual species [*Rogge et al.*, 1993]. Gas chromatography-mass spectrometry (GC-MS) has provided detailed speciation of insoluble compounds and those water-soluble compounds that can be derivatized [*Saxena and Hildemann*, 1996]. The concentrations of 49 organic compounds in aerosol over the western Atlantic Ocean have been identified, and most of the species that were detected are long-chain insoluble species [*Duce et al.*, 1983]. More polar substances, including dicarboxylic and ketocarboxylic acids, have also been identified in marine aerosol in the Pacific Ocean [*Kawamura and Gagosian*, 1990]. *Saxena and Hildemann* [1996] postulate that a significant part of the unidentified organic aerosol mass consists of water-soluble polar species. Hence, in addition to ambient measurements of the organic composition of sea salt aerosol our estimate of the complete composition (especially the polar constituents) will include compounds identified in seawater samples [*Riley and Chester*, 1971].

2.1. Measured Sea Salt Particle Organic Composition

Single particle measurements of sea salt aerosol suggest that organic species account for 5% to 50% of dry sea salt aerosol mass [*Middlebrook et al.*, 1998]. This concentration range is significantly higher than the organic fraction found in seawater, which is typically 0.01% of the total dry components in bulk seawater (most of which is NaCl) [*Riley and Chester,* 1971]. Studies of bubble bursting processes suggest that the formation of surface layers on seawater in which low surface tension species are enhanced may result in higher organic concentrations in the particles that form from bubble bursting [*Hoffmann and Duce*, 1976]. Laboratory work also suggests that even in well-mixed conditions, high molecular weight species may form particles preferentially during the film-breaking process [*Quinn et al.,* 1975]. Alternatively, this enhancement of the organic fraction of seawater may result from secondary organic condensation from the vapor phase, in which case, the composition of the organic species will be dependent on local atmospheric sources of biogenic and anthropogenic volatile organic compounds. In this work, we will only treat the simpler case, in which the organic species present in sea salt particles are assumed to be derived from seawater.

Field measurements have reported the carbon number and concentration ranges of long-chain nonpolar compound classes [*Gagosian et al.*, 1981; *Gogou et al.*, 1998]. Samples of marine aerosol were collected at Marshall Island in the western equatorial Pacific (11°20′N, 162°20′E) and Crete in the eastern Mediterranean (35°20′N, 25°42′E). Table 1 shows that the reported marine aerosol concentrations from different locations share a similar range of carbon number for the compounds identified.

Table 2. Composite Sea Salt Particle Composition Estimated From Direct Measurements of Marine Aerosol and From Seawater Composition

Chain Length	Fraction[a]	Compound Type	Fraction, %[b]	Species	Fraction, %[c]
Low molecular weight[d]	70%	malic acid	48	malic acid	48
		citric acid	22	citric acid	22
High molecular weight[d]	30%	monosaccharides	10	glucose	4.8
				fructose	4.7
		insoluble compounds	20	C25 alkane	0.073
				C27 alkane	0.15
				C29 alkane	0.19
				C31 alkane	0.15
				C33 alkane	0.073
				C24 alkanol	0.065
				C26 alkanol	0.28
				C28 alkanol	0.44
				C30 alkanol	0.28
				C32 alkanol	0.065
				C14 acid	1.8
				C15 acid	4.0
				C16 acid	5.2
				C17 acid	4.0
				C18 acid	1.8
				C22 acid	0.23
				C24 acid	0.83
				C26 acid	1.3
				C28 acid	0.83
				C30 acid	0.23

[a](Mass of each molecular weight)/(total organic mass).
[b](Mass of each type)/(total organic mass).
[c](Mass of each species)/(total organic mass).
[d]High molecular weight compounds are defined here as having molecular weights larger than 180 amu; low molecular weight compounds have molecular weights smaller than 180 amu.

Of the 49 organic species identified in direct measurements of sea salt particles, all are long-chain monofunctional compounds that tend to be insoluble [*Duce et al.*, 1983]. A small number of multifunctional compounds including diacids have been observed but account for less than $< 2\%$ of the observed organic mass [*Kawamura et al.*, 1996]. The majority of aerosol mass that is resolved into separate compound classes consists of alkanes, alkanols and acids. The common carbon number per molecule ranges roughly from 10 to 40 [*Gogou et al.*, 1998]. The concentration distribution of each of these compound classes with respect to carbon number generally peaks for compounds with 20 to 30 carbons per molecule with lower concentrations of both longer and shorter carbon chain compounds accounting for smaller mass fractions. The carbon number distribution in the estimated sea salt composition for insoluble compounds is provided in Table 2 from the measurements of *Gogou et al.* [1998] and *Gagosian et al.* [1981].

2.2. Seawater Organic Composition

Of the many organic species present in seawater, only long-chain alkanes, alkanols, and acids have been identified in sea salt aerosol. The identified fraction accounts for less than $< 10\%$ of the organic mass. The remaining fraction is likely to be similar in composition to the soluble compounds found in seawater, since these compound classes are difficult to analyze in ambient aerosol and are unlikely to decompose in aqueous solutions at atmospheric conditions. Consequently, our composite sea salt particle composition relies on seawater analysis for the estimated concentrations of soluble compounds.

Since we are interested in the relative fractions of each organic species that are present in seawater and most organic species are reported on an absolute basis, we need to first estimate the total fraction of organic mass in seawater. The basis for this calculation is the fraction of organic matter that is retained after ultrafiltration, so that organic matter larger than 0.2 μm is not included. This nonparticulate organic carbon content of ocean waters ranges from 0.3 to 1 mg [C] L^{-1} with the influence of geographical locations, seasons, and biological activities [*Menzel and Ryther*, 1970]. A typical value of 0.65 mg [C] L^{-1} is used here to represent the total organic carbon content of seawater. To convert from organic carbon mass to total organic mass, *Turpin and Lim* [2001] suggest average factors of 1.3 and 3.2 mg mg [C] $^{-1}$ for water-insoluble and water-soluble compounds, respectively. *Benner et al.* [1992] report that high molecular weight compounds account for 25% to 35% of total nonparticulate organic mass.

Using the average value of 30%, the remaining 70% of the total organic content consists of low molecular weight compounds. The assumptions that low molecular weight compounds are water-soluble and high molecular weight compounds are water-insoluble provide an estimated conversion factor of 2.2 mg mg $[C]^{-1}$ for seawater. The average organic mass in seawater is then ~ 1.4 mg L^{-1}.

Measurements of individual low molecular weight compounds reveal that high concentrations of malic acid (300 μg L^{-1} or 21% of the estimated nonparticulate organic mass) and citric acid (140 μg L^{-1} or 10% of the estimated nonparticulate organic mass) were observed along the Atlantic Coast [*Creac'h*, 1955]. Amino acids were measured to account for 10–25 μg L^{-1} in the Irish Sea (or 1% of the estimated nonparticulate organic mass) [*Riley and Segar*, 1970]. These three types of acids account for $\sim$ 31% of the nonparticulate organic mass, whereas 70% are expected to be low molecular weight compounds. The remaining 39% of low molecular weight compounds are thought to be similar compounds and so are modeled here by assuming that this measured ratio of malic acid to citric acid is appropriate for the entire low molecular weight fraction, such that malic acid is used to represent 48% of the organic mass and citric acid represents 22%.

Of the high molecular weight compounds, only the monosaccharides are soluble. *Benner et al.* [1992] report soluble carbohydrate concentrations up to 33%, although here we have used a more conservative estimate of 10%. Galactose, xylose, rhamnose, fucose, glucose, mannose, and arabinose have been measured in seawater in many locations around the world [*Aluwihare et al.*, 1997]. Since thermodynamic data for most of these sugars are unavailable, we have grouped them in two categories according to their solubility and have modeled each category using the properties of two well-studied sugars, fructose and glucose [*Velezmoro and Meirelles*, 1998; *Peres and Macedo*, 1997; *Comesana et al.*, 1999]. The very soluble compounds (galactose, rhamnose, mannose, xylose) account for about half of the monosaccharides present (4.7% of the total nonparticulate organic mass) and are represented by fructose because of its similar solubility and low deliquescence point. The slightly less soluble compounds (glucose, fucose, arabinose) account for the other half of the monosaccharides present (4.8% of the total nonparticulate organic mass) and are represented by glucose.

For insoluble compounds the concentration distributions of alkanes, alkanols, and acids are similar in seawater and sea salt particles. The seawater measurements are more complete and provide a better statistical representation of typical composition. The resulting model of sea salt aerosol composition is given in Table 2.

3. Thermodynamic Model

The development of this semiempirical organic-electrolyte model is described in detail by (Y. Ming and L.M. Russell, Thermodynamic equilibrium of aqueous solutions of organic-electrolyte mixtures in aerosol particles, submitted to *American Institute of Chemical Engineers Journal*, 2001, hereinafter cited as Y. Ming and L.M. Russell, submitted manuscript, 2001). At equilibrium, the Gibbs free energy (G) of the system will consist of contributions from chemical potentials (μ) of the components present in vapor and aerosol phases as well as from the surface tension (σ) over curved interfacial areas (a) between each of these phases. The equation describing this free energy is

$$G = \mu^{S} n^{S} + \mu^{L} n^{L} + \mu^{V} n^{V} + \sigma^{LV} a^{LV} + \sigma^{SL} a^{SL}, \quad (1)$$

where μ^{S}, μ^{L}, and μ^{V} are the chemical potentials of the solid, liquid, and vapor phases (assuming only one phase of each type), respectively, and n^{S}, n^{L}, and n^{V} are the numbers of moles of the solid, liquid, and vapor phases, respectively [*Mirabel et al.*, 2000]. For the soluble species studied here, water adsorbs to the solid surface below the deliquescence relative humidity, so we have assumed that the dry particle is coated with one or more layers of adsorbed water. The free energies at the solid/liquid (SL) and liquid/vapor (LV) interfaces are given by the products of their surface tensions σ^{SL} and σ^{LV} and the interfacial areas a^{SL} and a^{LV}. After dissolution of solid species, (1) reduces to

$$\begin{aligned} \mathrm{RH} &\equiv \frac{100 \times p_w(D_p)}{p_w^o} \\ &= 100 \times x_w \gamma_w \exp\left(\frac{4 M_w \sigma^{LV}}{RT \rho_w D_p}\right), \end{aligned} \quad (2)$$

where RH is the relative humidity of water vapor, p_w is the water vapor pressure in equilibrium with a particle of diameter D_p, p_w^o is the saturation vapor pressure of water, σ^{LV} is the surface tension at the liquid/vapor interface, x_w and γ_w are the mole fraction and activity coefficient of water in the aerosol phase, respectively, and M_w and ρ_w are the molecular weight and density at temperature T of the aqueous solution.

Most aerosol thermodynamic models describe aqueous solutions of electrolytes only [*Clegg et al.*, 1998]. Unlike electrolytes, organic species have diverse chemical structures and possess quite different attributes, both from each other and from electrolytes. The large number of organic species and the paucity of experimental data for the complex mixtures of organic and electrolyte species result in important uncertainties in their thermodynamic behavior.

3.1. Solution Activity

Two types of thermodynamic models have been developed to study the behavior of inorganic compounds in aqueous solutions: empirically correlated and excess Gibbs energy-based approaches. The Zdanovskii-Stokes-Robinson (ZSR) method is an example of an empirical approach [*Stokes and Robinson*, 1966]. Despite the simplicity and accuracy of empirical models, it is

impossible for the ZSR model to include organic compounds because the required empirical data on each organic component are prohibitively large. Excess Gibbs energy-based models such as the Pitzer model require expressions for the excess Gibbs energy of each compound in the mixtures. Experimental data are used to fit these parameters for differing concentrations. Using these fitted parameters, the predicted mixture properties compare well with the experimental data [*Pitzer*, 1991]. In some cases, the model can be extrapolated to make predictions for mixtures of which no measurements are available. For organic species, the UNIQUAC (Universal Quasi-Chemical)-based Functional-group Activity Coefficients model known as UNIFAC can be used to describe mixture properties [*Abrams and Prausnitz*, 1975; *Fredenslund et al.*, 1977]. Since the UNIFAC model is also based on expressions of excess Gibbs energy, our model combines Pitzer's equations and UNIFAC into a new model to describe solutions composed of ions, organic species, and water.

The effort to incorporate organic compounds into an aerosol thermodynamic model should address two kinds of interactions that are not considered in inorganic models: organic-water and organic-electrolyte interactions. The large number of organic species in sea salt aerosol can be treated as different combinations of functional groups. If it is assumed that the behavior of each functional group is independent of neighboring groups, the properties of complex organic mixtures result from several kinds of interacting groups. The approach of using functional groups as the main bodies of interaction in organic solutions, known as the Group Contribution Method (GCM) [*Reid et al.*, 1987], is the basis for several thermodynamic models, including UNIFAC. Different versions of UNIFAC are used widely for correlating experimental data and for predicting the behavior of unknown systems [*Fredenslund et al.*, 1977]. The existing parameter sets of UNIFAC were correlated primarily for nonaqueous organic mixtures typically important in chemical industries [*Gmehling*, 1995]. These parameter sets are fit to represent accurately properties of highly concentrated nonpolar systems of short-chain hydrocarbons and monofunctional compounds [*Wu and Sandler*, 1989, 1991; *Pividal and Sandler*, 1990]. Since our estimated sea salt aerosol composition includes long-chain monofunctional and short-chain multifunctional substances, we have revised the correlation by creating additional "multifunctional groups."

The activity coefficient varies with particle composition, namely, the mole fraction x_m of a species m, where

$$x_m = \frac{n_m}{n_w + \sum_o n_o + \sum_i n_i}. \tag{3}$$

The subscripts w, o, and i of mole number n represent water, organic compound, and ion, respectively. The summations are over all organic species and ions. Because the contributions of interactions between species are additive, the activity coefficients of species in solution can be expressed as the sum of long-range (LR), short-range (SR) and UNIFAC-based organic (U) interactions [*Li et al.*, 1994].

$$\ln \gamma_m = \ln \gamma_m^{\mathrm{LR}} + \ln \gamma_m^{\mathrm{SR}} + \ln \gamma_m^{\mathrm{U}}. \tag{4}$$

In (4), m refers to any species in solution (ions, water and organic species). The long-range and short-range parts come from the interaction between water and ions [*Clegg et al.*, 1992]. The long-range effect is the dominant term for dilute aqueous solutions of electrolytes. With increasing concentrations of ions, the short-range effect dominates the activity coefficients. The interactions between ions and organic compounds and between water and organic compounds are described by the UNIFAC contribution.

3.1.1. Electrolyte-water interactions. In the mole fraction based Pitzer equations [*Clegg et al.*, 1992] the activity coefficients have two parts: the long-range and short-range interactions between water and ions. These long-range and short-range effects depend on water and ion interactions only and so are taken to be independent of the organic species present. Hence Pitzer's equations are used to compute the corresponding contributions to the activity coefficients as given by *Clegg et al.*'s [1992] equations (24)–(26) for $\ln \gamma_m^{LR'}$ and equations (15)–(17) for $\ln \gamma_m^{SR'}$, in which we have used the inorganic mole fraction x'_m where

$$x'_m = \frac{n_m}{n_w + \sum_i n_i} \tag{5}$$

and m may be either water or an ion. Binary and ternary interaction parameters required for these equations are taken from *Clegg et al.* [1998]. To convert these activity coefficients from the inorganic mole fraction basis x'_m to the actual mole fractions, we employ the translation

$$\ln \gamma_m^{\mathrm{LR}} = \ln \gamma_m^{\mathrm{LR}'} - \ln \left(1 - \sum_o x_o\right) \tag{6}$$

$$\ln \gamma_m^{\mathrm{SR}} = \ln \gamma_m^{\mathrm{SR}'} - \ln \left(1 - \sum_o x_o\right) \tag{7}$$

to calculate the effective activity coefficients in the mixed organic-electrolyte solution.

3.1.2. Organic-water interactions. In UNIFAC, all neutral molecules are treated as combinations of different groups. The behavior of a specific group is assumed to be independent of its surrounding groups. Thus the interaction parameters correlated from experimental data of known systems can be used to predict unknown systems. This extrapolation is more reliable when the chemical structures of components in unknown systems are similar to known systems because the assumption about the independence of groups holds better in this situation. The equations describing the UNIFAC model are given by *Fredenslund et al.* [1977].

Existing versions of UNIFAC can be used to predict the properties of multifunctional compounds from

Table 3. Group Interaction Parameters Used to Calculate Organic Water Interactions by the UNIFAC Approach.[a]

	Na^+	Cl^-	$-CH_n$[b]	-OH[c]	-COOH[d]	$-CH_nCO$[e]	$-CH_n$[f]	$-CH_nO$[g]	-OH[h]	$-CH_n$[i]	-COOH[j]	-OH[k]	H_2O
Na^+	0	0	7794[l]	6654[l]	6654[l]	6654[l]	376[l]	203[l]	147[l]	2292[l]	1958[l]	1849[l]	0
Cl^-	0	0	8093[l]	53760[l]	53760[l]	53760[l]	719[l]	638[l]	366[l]	2623[l]	2289[l]	2180[l]	0
$-CH_n$[b]	7771[l]	8107[l]	0	986.5	663.5	476.4	0	251.5	986.5	0	663.5	986.5	1318[l]
-OH[c]	5768[l]	7032[l]	156.4	0	199	84	156.4	28.06	0	156.4	199	0	1000[l]
-COOH[d]	5768[l]	7032[l]	315.3	-151	0	-297.8	315.3	-338.5	-151	315.3	0	-151	1000[l]
$-CH_nCO$[e]	5768[l]	7032[l]	26.76	164.5	669.4	0	26.76	5.202	164.5	26.76	669.4	164.5	1000[l]
$-CH_n$[f]	636[l]	1027[l]	0	986.5	663.5	476.4	0	251.5	986.5	0	663.5	986.5	1318
$-CH_nO$[g]	-640[l]	-720[l]	83.36	237.7	664.6	52.38	83.36	0	237.7	83.36	664.6	237.7	2007[l]
-OH[h]	184[l]	488[l]	156.4	0	199	84	156.4	28.06	0	156.4	199	0	-189.7[l]
$-CH_n$[i]	1008[l]	1491[l]	0	986.5	663.5	476.4	0	251.5	986.5	0	663.5	986.5	1318
-COOH[j]	-23.3[l]	-123.1[l]	315.3	-151	0	-297.8	315.3	-338.5	-151	315.3	0	199	-163.3[l]
-OH[k]	208.8[l]	781.6[l]	156.4	0	199	84	156.4	28.06	0	156.4	-151	0	-92.3[l]
H_2O	0	0	541.3[l]	-959[l]	-530[l]	-471[l]	300	193.1[l]	171.3[l]	300	64.6[l]	224.4[l]	0

[a] *Fredenslund et al.* [1977].
[b] $-CH_n$ (n=0,1,2,3) in long-chain monofunctional compounds.
[c] -OH in long-change monofunctional compounds.
[d] -COOH in long-change monofunctional compounds.
[e] $-CH_nCO$ (n=2,3) in long-change monofunctional compounds.
[f] $-CH_n$ (n=0,1,2,3) in monosaccharides.
[g] $-CH_nO$ (n=0,1,2) in monosaccharides.
[h] -OH in monosaccharides.
[i] $-CH_n$ (n=0,1,2,3) in hydroxy-acids.
[j] -COOH in hydroxy-acids.
[k] -OH in hydroxy-acids.
[l] Correlated by Y. Ming and L.M. Russell (submitted manuscript, 2001) from experimental data of *Kojima et al.* [1997], *Xie et al.* [1997], *Velezmoro and Meirelles* [1998], *Peres and Macedo* [1997], *Herz and Hiebenthal* [1929], and *Comesana et al.* [1999]; all other parameters were correlated by *Gmehling et al.* [1982].

the interaction parameters between groups derived from monofunctional compounds for which there are experimental data [*Pividal and Sandler*, 1990]. However, in practice, this approach cannot provide reasonable representations of multifunctional compounds with the same accuracy as for monofunctional compounds [*Wu and Sandler*, 1989, 1991]. The reason for its poor performance is that the UNIFAC assumption of independence of functional groups does not hold for neighboring polar functional groups in the same molecule. To improve the prediction of the behavior of multifunctional organic species, we introduce new groups specifically for different types of multifunctional compounds in which we have paired adjacent functional groups into single "multifunctional" groups. The interaction parameters of these groups are utilized to predict the behaviors of substances with similar multifunctional structures. All of the soluble organic compounds in our estimated sea salt particle composition are multifunctional. Since the parameter sets of existing UNIFAC models were derived from and thus are only accurate for monofunctional substances, experimental data for the multifunctional compounds present in sea salt aerosol (mainly sugars and hydroxy acids) were used to fit a new set of interaction parameters for several additional multifunctional groups (for example, combined -OH and -COOH). The new parameters fit malic acid, citric acid, and glucose data to within 3%.

Interactions between inorganic ions and organic compounds in UNIFAC are included by introducing ionic groups. Since the long- and short-range interactions are calculated from the long- and short-range terms in (7), there are no additional interactions that must be accounted for by UNIFAC, so the UNIFAC parameters describing ion and water interactions with each other are set to zero, similar to the self-consistent approach proposed by Clegg et al. [2001]. Interaction parameters between ionic and organic groups are incorporated as UNIFAC interactions using the method of *Xie et al.* [1997]. Thermodynamic data from the literature were used to describe electrolyte-organic interactions [*Kojima et al.*, 1997; *Xie et al.*, 1997; *Velezmoro and Meirelles*, 1998; *Peres and Macedo*, 1997; *Herz and Hiebenthal*, 1929; *Comesana et al.*, 1999]. The fitted parameters used in UNIFAC to describe both multifunctional compounds and electrolytes are compiled in Table 3.

3.2. Phase Equilibrium

Using this algorithm to calculate the activity coefficients, we then determine the most favored free energy configuration that satisfies (1). In doing this, the algorithm also allows for solid and liquid phases to form in addition to the aqueous phase. The differences in polarity of electrolytes, organic compounds, and water tend to encourage the formation of more than two phases at low relative humidities, each phase containing substances of similar polarity level. Particle water content influences the distribution of other aerosol components

among possible phases and therefore dictates the water activity in solution.

The total mass of each component present in the system (in all liquid, solid, and vapor phases) is fixed from our estimated sea salt organic composition. Then the corresponding amount of water is allowed to vary during the optimization. The solid phases include pure organic species and all forms of inorganic salts that can be formed from the ions present. The distribution of species among phases is determined by minimizing the total Gibbs free energy of the system. This energy is described for single homogeneous solid, liquid, and vapor phases in equilibrium in (1). Expressing (1) explicitly in terms of the contributions from the species present in each of these phases and allowing multiple liquid and solid phases to be present results in

$$\begin{aligned} G &= \sum_s \left(\sum_i \mu_i^s n_i^s + \sum_o \mu_o^s n_o^s \right) \\ &+ \sum_l \left(\sum_i \mu_i^l n_i^l + \sum_o \mu_o^l n_o^l + \mu_w^l n_w^l \right) + \mu_w^{\mathrm{V}} n_w^{\mathrm{V}} \\ &+ \sum_l \sigma^{l\mathrm{V}} a^{l\mathrm{V}} + \sum_l \sum_s \sigma^{sl} a^{sl}, \end{aligned} \tag{8}$$

where s denotes a solid phase, l denotes a liquid phase, and V denotes the vapor phase. The reference states of the organic and ion species is solid, whereas the reference state for water is vapor. Equation (8) can be simplified by noting that the reference states of the chemical potentials cancel and that the phase changes can be described by ratios of fugacities or equilibrium constants to obtain the change in Gibbs free energy

$$\begin{aligned} \Delta G &\equiv G - G^o \\ &= RT \sum_l \sum_i \ln \left(\frac{x_i^l \gamma_i^l}{\bar{x}_i^l \bar{\gamma}_i^l} \right) n_i^l \\ &+ RT \sum_l \sum_o \ln \left(\frac{x_o^l \gamma_o^l}{\bar{x}_o^l \bar{\gamma}_o^l} \right) n_o^l \\ &+ RT \sum_l \ln \left(\frac{x_w^l \gamma_w^l}{\mathrm{RH}/100} \right) n_w^l \\ &+ \sum_l \sigma^{l\mathrm{V}} a^{l\mathrm{V}} \\ &+ \sum_l \sum_s \sigma^{sl} a^{sl}, \end{aligned} \tag{9}$$

where o and i denote organic and ionic species in solid and liquid phases (Y. Ming and L.M. Russell, submitted manuscript, 2001). The variables n_k^l, x_k^l, and γ_k^l are the mole number, mole fraction, and activity coefficient in liquid phase l; $\bar{x}_k^l$ and $\bar{\gamma}_k^l$ are the mole fraction and activity coefficient in liquid phase l at saturation. The ratio of liquid-to-solid reference fugacities, $f_o^{\mathrm{L}}/f_o^{\mathrm{S}}$ quantifies the energy of melting pure organic o from solid to liquid. Traditionally, the term fugacity ratio is only used with organic compounds; for salts the same property is defined as the equilibrium constant at the solubility limit K_i^{eq}. In other words, we use

$$\frac{f_i^{\mathrm{L}}}{f_i^{\mathrm{S}}} = K_i^{\mathrm{eq}} \tag{10}$$

where the solublities are calculated using *Clegg et al.* [1998]. The genetic optimization algorithm GENOCOP III [*Michalewicz and Nazhiyath,* 1995] then searches for the minimum value of G, subject to nonnegative concentrations and conservation of mass of each component.

3.3. Surface Tension Algorithm

Surface tension increases the relative humidity required to be in equilibrium with the water in the particle. The dissolution of salts and organic compounds alters the surface tension of an aqueous solution [*Li et al.*, 1994]. Electrolytes increase the surface tension, but many organic compounds lower the surface tension.

The solution present in aerosol can be divided into a surface phase and a bulk phase. The surface phase is the thin layer immediately adjacent to the gas phase, so the pressure there is equal to atmospheric pressure. The mass occupied by the surface phase is assumed to be negligibly small relative to the bulk phase and the composition of the surface phase is assumed to be independent from that of the bulk phase. Equilibrium of organic species o at the interface between the surface and bulk phases then requires that

$$\sigma = \sigma_o + \frac{RT}{A_o} \ln \frac{x_o^{\mathrm{S}} \gamma_o^{\mathrm{S}}}{x_o^{\mathrm{B}} \gamma_o^{\mathrm{B}}}, \tag{11}$$

where σ and σ_o are the surface tension of the solution and pure organic species o, respectively [*Nath*, 1999]. Surface tensions for pure species are calculated according to *Lyman et al.* [1990]. The parameters γ_o^{S} and γ_o^{B} are the activity coefficients of o in the surface and bulk phases, respectively, and x_o^{S} and x_o^{B} are the mole fractions of o in the surface and bulk phases. A_o is the molar surface area of organic component o. The concentrations of electrolytes in the surface phase are assumed to be proportional to those in the bulk phase using constants correlated from experimental data:

$$x_i^{\mathrm{S}} = k_i x_i^{\mathrm{B}}, \tag{12}$$

where k_i is measured experimentally for each species [*Li et al.*, 1994]. The surface tension is then determined from experimental data for a solution with composition x_i^{S}.

4. Predicted Hygroscopic Growth of Sea Salt Particles

Particle hygroscopic growth describes water uptake from the vapor phase by soluble substances present in particles. The hygroscopic growth factor (GF) serves as a quantitative description of the amount of water taken up using a ratio of the diameter at ambient humidity ($D_{p,\mathrm{RH}}$) relative to the original dry particle size ($D_{p,\mathrm{dry}}$) and is given by *Hämeri et al.* [2000] as

$$\mathrm{GF(RH)} = \frac{D_{p,\mathrm{RH}}}{D_{p,\mathrm{dry}}}. \tag{13}$$

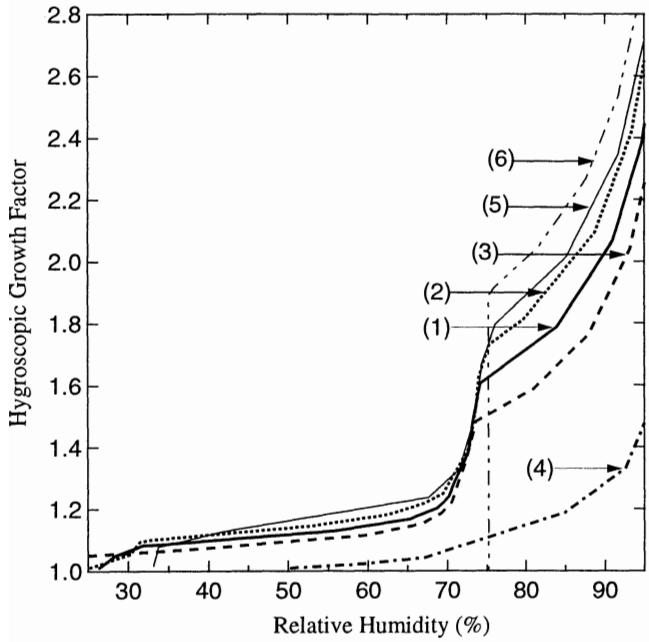

Figure 1. Predicted hygroscopic growth for bulk solutions of varying organic composition. The compositions studied are (1) 30% organic species and 70% inorganic salts (base case, solid line), (2) a lower organic content case of 10% organic species and 90% inorganic salts (dashed-dotted-dotted line), (3) a higher organic content case of 50% organic species and 50% inorganic salts (dashed line), (4) 100% organic species (dashed-dotted line), (5) 100% inorganic salts found in seawater (thin solid line), and (6) 100% NaCl (thin dotted line).

In hygroscopic growth factor measurements the relative humidity is lowered below the efflorescence point to dry out the particles, and then the humidity is increased to obtain the dependence of particle growth factors as relative humidity increases [*Cruz and Pandis,* 2000].

To describe this complex mixture, we have made a series of assumptions about sea salt particles based on incomplete data about their composition. In this section we use these simplifications to study this simplified behavior for sea salt particle mixtures in bulk solutions and in particles of different sizes. All of the experimental data used here were measured at 298 K, so the predictions here are only accurate near 298 K because the model does not include parameterizations of the temperature dependence of the solution properties. Section 4.1 evaluates these assumptions, the accuracy of the limited data available, and their importance to our conclusions. These simplifications to describe sea salt particle chemical equilibria are that (1) insoluble species exist in particles as independent solid phases that adsorb a negligible amount of water, (2) secondary inorganic components of seawater (Mg^{2+}, Ca^{2+} and SO_4^{2-}) have negligible interactions with organic species, and (3) insoluble organic compounds in sea salt are represented by the molecular weight and density of the range of alkanes, acids, and alcohols in Table 2; soluble organic compounds in sea salt are represented by the molecular weight, density, solubility, activity, and surface tensions of the mixture of malic acid, citric acid, glucose, and fructose given in Table 2.

In addition, we assume here that sea salt formation mechanisms are chemically homogeneous, such that sea salt particles present in the atmosphere are internal mixtures representative of the estimated organic (and inorganic) composition. Few data are available to evaluate this assumption for sea salt, but a comparison of internally mixed and externally mixed aerosol growth shows few differences (Y. Ming and L.M. Russell, submitted manuscript, 2001).

4.1. Sea Salt Organic Species in Bulk Solutions

These assumptions constrain the equilibrium behavior of the mixture, providing a description of the internally mixed behavior of sea salt particles. Organic species provide some additional ions that dissolve below the deliquescence point of sodium chloride but also some insoluble material that does not dissolve at all (even though they may be present in particles that do take up water). The net effect is to create particles that take up more water at lower humidities but less water overall than either a pure sodium chloride or a strictly inorganic seawater solution. In this study, the basis for comparison is taken to be constant dry mass of both soluble and insoluble components (that is, all nonwater mass).

This section considers the case of a bulk quantity of solution, namely, one in which the interfacial energy contribution on a mass basis is negligible because the particle diameter is effectively infinite (and hence the amount of interfacial area relative to the volume of the "particle" is small). In the system studied here, we approach this limit for diameters > 1000 nm.

4.1.1. Sea salt with 30% organic composition. Figure 1 shows the hygroscopic growth of the sea salt mixture that includes 30% of the estimated organic composition. The comparison shows differences in water uptake below and above 75% (NaCl deliquescence) compared to inorganic sea salt (with 0% organic composition). Both curves take up water below 75%, although the 30% organic case has a higher initial hygroscopic growth since fructose dissolves at 62% relative humidity. In addition, the internal mixture of organic species and inorganic salts takes up more water than the sum of both species independently because of the organic-electrolyte interactions [*Andrews and Larson,* 1993; *Hansson et al.,* 1998].

At 75% relative humidity the sodium chloride that constitutes the majority of the solute present dissolves resulting in a steeply sloped hygroscopic growth curve. Above this relative humidity the hygroscopic growth is significantly lower than both pure sodium chloride and 15% lower than inorganic seawater because 9% of the dry mass consists of insoluble organic compounds and 15% consists of the remaining soluble compounds citric acid, glucose, and malic acid. These three soluble com-

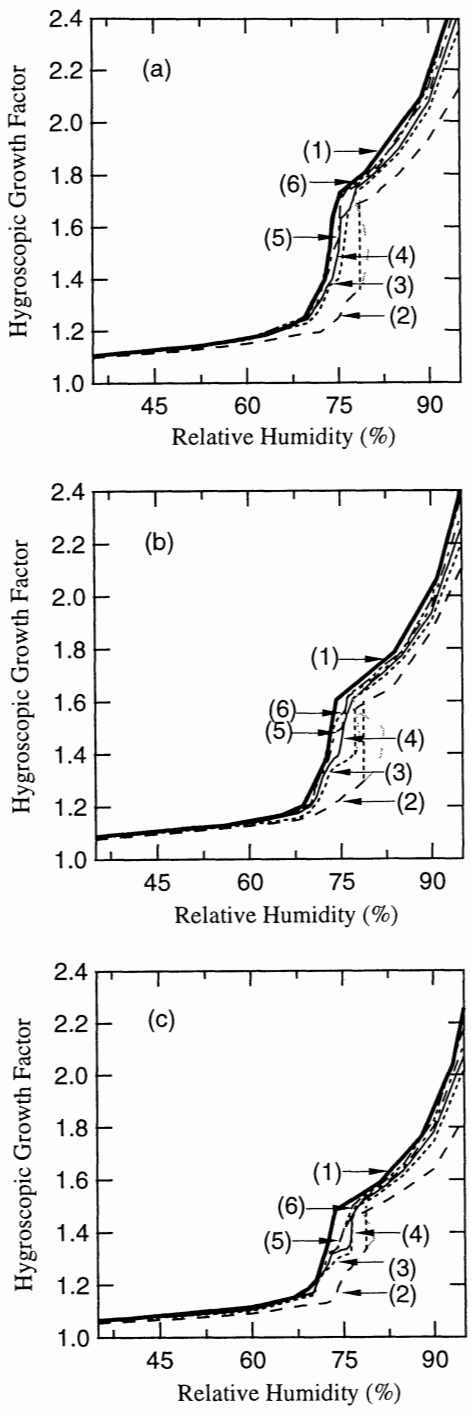

Figure 2. Predicted hygroscopic growth of particles with varying dry diameters at organic contents of (a) 10%, (b) 30%, and (c) 50%. The dry diameters shown are (1) bulk case (thick solid line), (2) 15 nm (dashed line), (3) 35 nm (dashed-dotted-dotted line), (4) 50 nm (thin solid line), (5) 75 nm (dashed line), and (6) 165 nm (dotted line). For curves with multiple equilibria near deliquescence, shaded lines show the deliquescence path and shaded dotted lines show unstable equilibria.

pounds dissolve as relative humidity increases, at 84%, 86%, and 87%, respectively. Above this relative humidity only the very insoluble compounds remain undissolved, resulting in lower hygroscopic growth than the strictly inorganic salt composition.

4.1.2. Varied organic composition. Since the fraction of sea salt particles that consists of organic species has not been well characterized by measurements and also will vary with local seawater concentrations, Figure 1 also compares the influence of differing fractions (10% and 50%) of the same estimated organic composition to the base case composition of 30% organic. The 10% organic case is within 5% of the hygroscopic growth of the inorganic sea salt composition, so that few differences would be discernible by measurement techniques. The 50% organic case has 25% less growth than the inorganic case.

In this comparison we have kept the relative concentration of each organic species constant. As a consequence, the fraction of organic mass that dissolves at each successive deliquescence point is similar, thus maintaining the shape of the hygroscopic growth curves but shifting them to lower magnitudes as the organic fraction (and hence the insoluble mass) is increased. If the types and relative amounts of organic species are also varied, then the qualitative features of the hygroscopic growth curve also change. The effect of changing the composition of the estimated sea salt organic fraction is discussed in section 5.3.

4.2. Sea Salt Particle Size-Dependent Behavior

In order to extend the model to the behavior of particles of specific submicron diameters, the interfacial energy terms in (9) become important. Figure 2 illustrates that for a given composition and relative humidity, a smaller particle will take up less water than a larger particle. For atmospheric aerosol particles the range of diameters for which this model applies is 5 to 1000 nm. Above 1000 nm the effect of surface tension is negligible for the compositions and relative humidity ranges of interest here. Below 5 nm the size-independent bulk surface tension on which (9) relies may not accurately represent the submacroscopic molecular interactions among the finite number of molecules in these clusters [*Girshick and Chiu,* 1990; *Wilemski,* 1995].

Particles of 165 nm diameter differ by $< 5\%$ from the bulk solution. Decreasing the diameter to 75 and 50 nm shows additional decreases in hygroscopic growth, but for dry particle sizes of 35 and 15 nm the shape of the curve in the deliquescence region shifts from positively sloped past vertical to negatively sloped. This slope is caused by the surface tension of the liquid/vapor interface competing with the dissolution of NaCl after reaching the solubility limit. The negative slope results in three predicted equilibria for a small range of relative humidities near the deliquescence point, where the third equilibrium is the partially wet particle (and the first two are the dry and wet states).

Deliquescence is predicted to occur when the Gibbs free energy of the wet particle (as given by equation (1)) is less than that of the dry particle. For the mixtures studied here, the sodium chloride as well as other species will adsorb water prior to deliquescence such

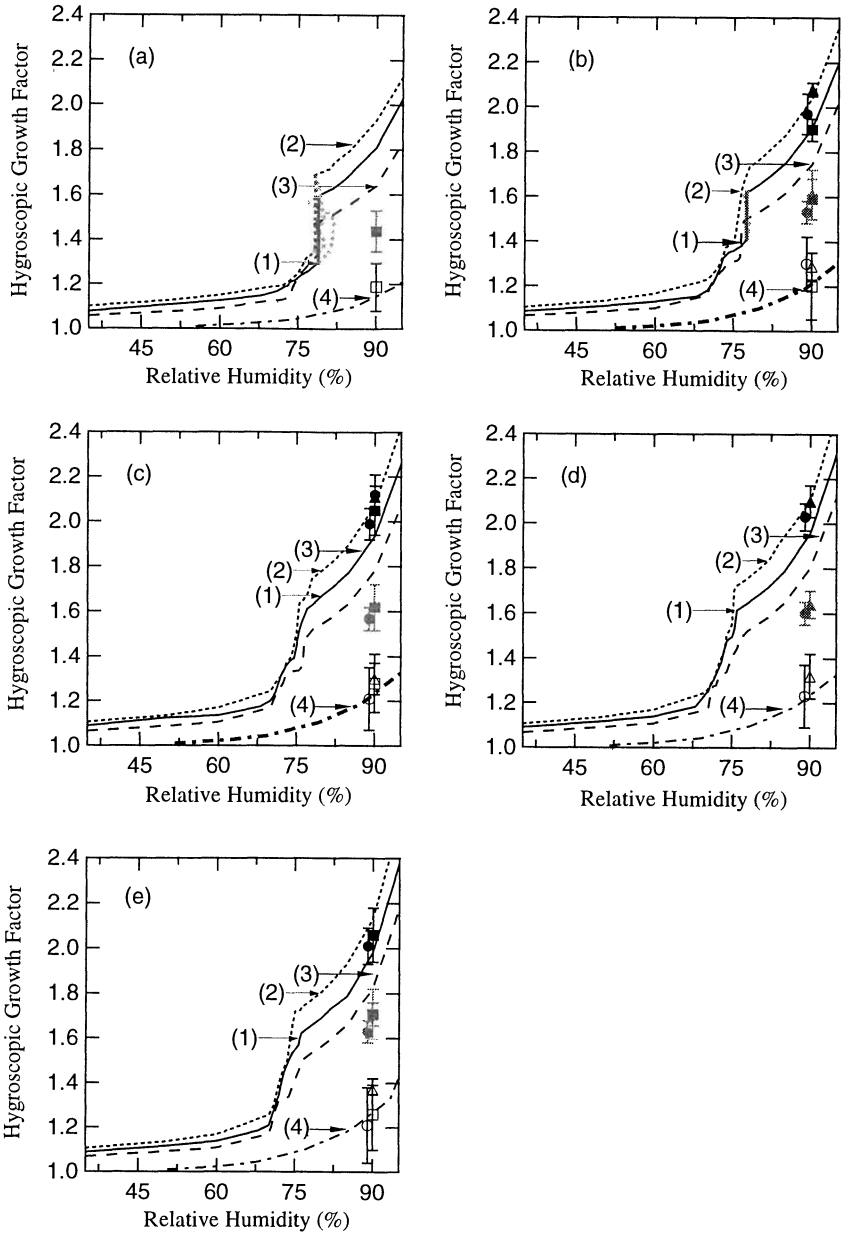

Figure 3. Predicted hygroscopic growth of particles with varying organic contents at a range of particle sizes. The sizes shown are (a) 15 nm, (b) 35 nm, (c) 50 nm, (d) 75 nm, and (e) 165 nm. The compositions shown are (1) 30% organic species and 70% inorganic salts (base case, solid line), (2) a lower organic content case of 10% organic species and 90% inorganic salts (dashed-dotted-dotted line), (3) a higher organic content case of 50% organic species and 50% inorganic salts (dashed line), and (4) a 100% organic content case (dashed-dotted line). For curves with multiple equilibria near deliquescence in Figures 3a and 3b, shaded lines show the deliquescence path and shaded dotted lines show unstable equilibria. In addition, the plot illustrates recent measurements of ambient particle growth from field project data reported by *Berg et al.* [1998] (ACE1, triangles), *Swietlicki et al.* [2000] (ACE2, circles), and *Zhou et al.* [2001] (AOE, squares). The particles were grouped by those authors as particles similar to sea salt (solid symbols), particles that are more hygroscopic than sulfate (shaded symbols), and particles that are less hygroscopic than sulfate (open symbols). The error bars on the symbols indicate the standard deviation for each category during the project.

that the dry particle will be coated with a layer of water [*Peters and Ewing,* 1997a, 1997b; *Foster and Ewing,* 1999, 2000]. Since we have used experimental data from bulk surfaces to describe adsorption onto particles of finite diameters, we have omitted here contributions from the disjoining pressure of the initial aqueous film on the particle surface [*Israelachvili,* 1996; *Adamson,* 1990]. Preliminary experiments of water adsorption on small particles show that water will adsorb on particles smaller than 400 nm, but there is some evidence

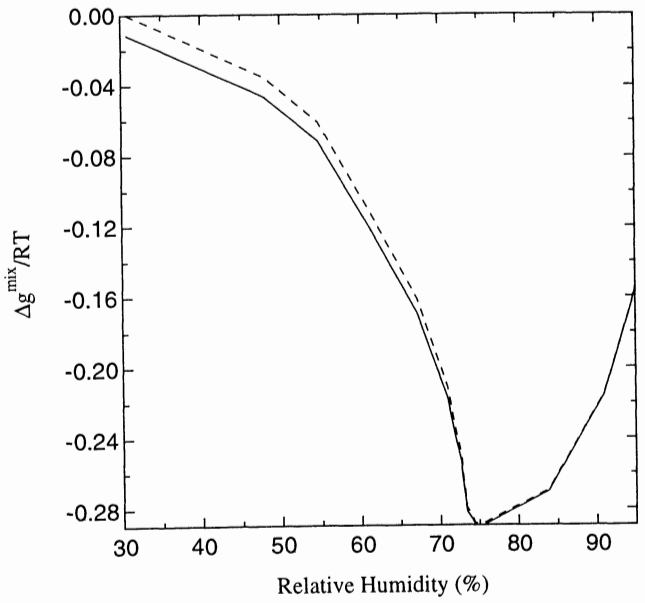

Figure 4. Gibbs free energy of system phase equilibrium for individual solid phases for undissolved component (dashed line) and for a nonaqueous phase liquid mixture of undissolved organic species (solid line).

that the amount adsorbed below the deliquescence relative humidity is enhanced over a bulk surface [*Weis and Ewing*, 1996]. Clearly more experimental studies are needed to evaluate this approach.

The straight vertical line for each case in Figure 3a shows the relative humidity at which the wet particle free energy drops below the dry. The free energy of the partially wet state is higher than both the wet and dry states at all relative humidities, so this state represents an unstable equilibrium. Since the mixtures here include compounds (e.g., magnesium sulfate) which take up water below 70% relative humidity, the "dry" state will include some water associated with components other than NaCl. For example, for 15 nm sea salt particles with 10% organic composition, deliquescence occurs at 78% relative humidity when the free energy of the wet particle has decreased to $3.50 \times 10^{-20} \times RT$, which is just below the free energy of the dry particle at $3.56 \times 10^{-20} \times RT$ (at lower relative humidities, the free energy of the wet particle is higher than the dry particle). At this relative humidity the free energy of the partially wet particle is $3.65 \times 10^{-20} \times RT$, so that it is less stable than both dry and wet states. *Russell and Ming* [2001] discuss the stability of these partially wet states in detail, as well as the sensitivity of this result to the value of the solid/liquid surface tension. For the sea salt mixtures described here, in the absence of data for solid/liquid surface tensions for other species, the solid/liquid interface is approximated by measured values for NaCl ($\sigma^{SL} = 29$ mN m^{-1}) and the liquid/vapor interface is calculated as a mixture of saturated NaCl solution ($\sigma^{LV} = 83$ mN m^{-1}) with contributions from dissolved organic species calculated as described in section 3.3.

The same trends are seen in all of the particle sizes shown, including a jump in water uptake that occurs in each curve when the remaining NaCl dissolves as the relative humidity reaches 75%. Outside of the relative humidities near the deliquescence region in which rapid growth occurs, the hygroscopic growth decreases almost linearly with dry particle sizes between 165 and 15 nm.

4.3. Comparison to Measured Hygroscopic Growth of Ambient Particles

Berg et al. [1998], *Swietlicki et al.* [2000], and *Zhou et al.* [2001] have measured the hygroscopic growth of ambient particles in marine environments in the Southern Ocean, the northeastern Atlantic Ocean, and the Arctic Ocean, respectively. Their results are consistent with the presence of two or more types of particles, one of which was frequently similar in growth characteristics to sea salt. Another particle type that appeared frequently (classified in the above studies as "less hygroscopic") seemed to have low water uptake properties that would be similar to particles that were primarily composed of organic species. Their measured hygroscopic growth factors for particles of 15, 35, 50, 75, and 165 nm in diameter are illustrated in Figure 3.

Figure 3b shows that for 35-nm-diameter measurements the particle classes identified as "sea salt" had hygroscopic growth properties similar to inorganic sea salt mixed with between 10% and 30% organics. The Arctic Ocean results are almost identical to the 30% organic case, while the northeastern Atlantic Ocean sea salt particles measured during ACE2 have < 10% organic compounds and are only slightly less hygroscopic than is predicted for pure inorganic sea salt (with 0% organics). For 50-nm particles in Figure 3c and 75-nm particles in Figure 3d the 10% organic case provides a good prediction of the hygroscopic growth, but the 165-nm case in Figure 3e has a lower hygroscopic growth that compares better with the growth for ~ 20% organic compounds. The error bars show that the reported uncertainty in the measurement is comparable to the difference between the 10% and 30% organic cases, limiting our ability to draw more specific conclusions. An alternative interpretation is that some non-sea-salt sulfate was also present that would reduce the hygroscopic growth. Since particle composition measurements associated with each of these particle types are not available, this comparison serves only to highlight the consistency of the measurements with sea salt particles containing organic species.

In addition, the northeastern Atlantic Ocean and Arctic Ocean samples that included the particle type identified as "less hygroscopic" [*Swietlicki et al.*, 2000; *Zhou et al.*, 2001] are consistent with a 100% mixture of the estimated sea salt organic composition (with no inorganic ions present). While there are certainly infinite combinations of organic species that yield similar hygroscopic behavior, this result does suggest that this type of particle is consistent with ocean-derived organic

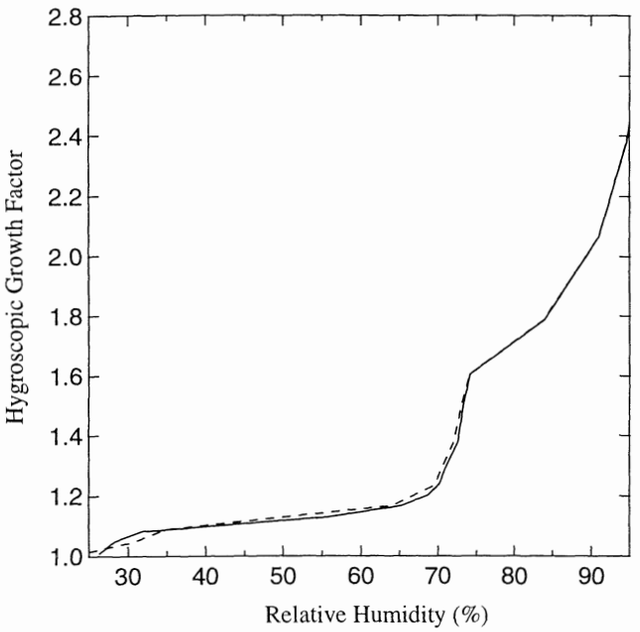

Figure 5. Effect of organic-electrolyte interactions for secondary inorganic ions (Mg^{2+}, SO_4^{2-}, and Ca^{2+}) on hygroscopic growth. The hygroscopic growth for the base case composition (30% organics and 70% inorganic salts) was calculated assuming (1) that these secondary ions had no interactions with organic species (solid line) and (2) that each secondary inorganic ion had twice the "salting-out" effect of Na^+ or Cl^- (dashed line).

particles that have little or no inorganic salts present.

The hygroscopic growth measurements also frequently reported a "more hygroscopic" category of observed particle growth. The "more hygroscopic" type particles are likely to include a significant fraction of ammonium sulfate based on the presence of both ammonium and sulfate ions in associated bulk filter measurements [*Quinn et al.*, 1998; 2000]. Nonetheless, these calculations indicate that the hygroscopic growth measured would also be consistent with a mixture of sea salt with $\sim 50\%$ marine organic species. The variability indicated by the bounds of the whiskers on the measured hygroscopic growth values shows that there was a significant standard deviation in the hygroscopicities of the particles measured in each field project. This variability suggests that different compositions of particles were found on different days.

5. Model Uncertainties

Testing the model sensitivity to assumptions and its uncertainties with experimental data challenges the robustness of our conclusions. We have calculated the equilibria predicted when each of our assumptions is relaxed. This approach includes the neglect of interactions of nonNaCl inorganic ions with organic species, the estimated organic composition, the presumed internal mixing of sea salt particle components, and the phase state of nonaqueous components. In addition, we have estimated the model error propagated by the experimental errors in data used to make our empirical parameterizations. This calculation serves to provide an indication of the most important measurements needed to reduce the uncertainties in the hygroscopic growth.

5.1. Sensitivity to Nonaqueous Particle Phases

To facilitate the search for the minimum free energy configuration that satisfies equation (9), it is convenient to constrain the components or parts of components that do not dissolve into separate solid or liquid phase as determined by their pure component properties. Since excess properties are not additive, the assumption does not hold for combinations of organic solids that can form liquids because the mixture melting point is lower than any of the melting points of the individual solids [*Peters et al.*, 2000]. Relaxing this assumption showed that the insoluble organic mixture described in Table 2 will form a nonaqueous phase liquid (NAPL) and that this configuration results in a lower Gibbs free energy for the system, as illustrated in Figure 4.

The hygroscopic growth properties of the particles that include NAPL states are identical to the configuration with solid organic species since neither the solids nor the NAPL components take up water. Small changes are predicted for the particle density and surface interactions, although these considerations are arguably more dependent on the morphology and mixing homogeneity (which have not been considered here).

5.2. Sensitivity to Inorganic Ion Interactions With Organic Species

Including the electrolyte-organic interactions following the approach of *Xie et al.* [1997] requires experimental data for the activity coefficients of the electrolyte with a range of organic compounds, as discussed by (Y. Ming and L.M. Russell, submitted manuscript, 2001). Since these data are not currently available for the secondary inorganic ions present in seawater (namely, Mg^{2+}, Ca^{2+}, and SO_4^{2-} ions), the organic-electrolyte interactions for these species have been neglected in the preceding hygroscopic growth calculations. We have estimated the magnitude of the error incurred by this assumption by comparing the growth factors with (1) no organic-electrolyte interactions for Mg^{2+}, Ca^{2+}, and SO_4^{2-} ions or (2) treating each Mg^{2+}, Ca^{2+}, and SO_4^{2-} ion as two additional Na^+ or Cl^- ions. The latter scenario considers a "worst-case" scenario in which the "salting out" effect of sulfate ions are double that of each chloride ion. Figure 5 shows that because sulfate accounts for only 3.5% of the inorganic salt mass there is less than a 2% difference between the two assumptions in the deliquescence region and negligible differences elsewhere.

Even though these secondary inorganic ions account for $\sim 15\%$ of the total ions in sea salt, the interactions of these ions with different classes of organic compounds has only a small effect on the predicted growth accord-

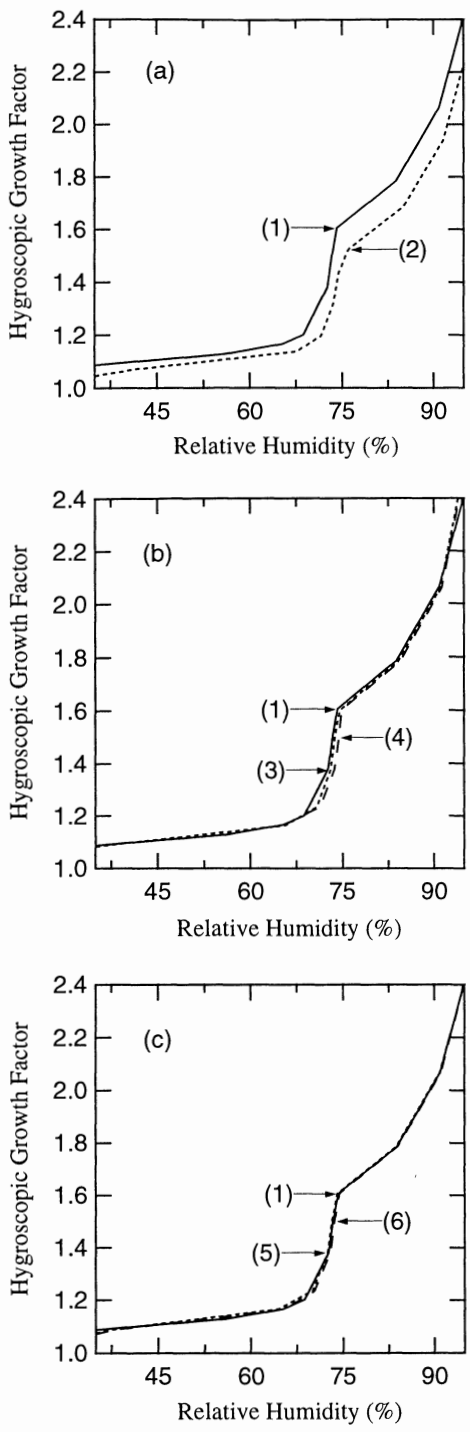

Figure 6. Sensitivity of predicted hygroscopic growth to different organic species for (a) insoluble organic components, (b) sugars, and (c) organic acids. Base case of (1) 30% organics and 70% inorganic salts (solid line) is compared to an all-insoluble case with (2) 30% insoluble organics and 70% inorganic salts (dotted line) (Figure 6a); an all-glucose case with (3) 24% glucose, 6% insoluble organics, and 70% inorganic salts (dotted line) and an all-fructose case with (4) 24% fructose, 6% insoluble organics, and 70% inorganic salts (dashed line) (Figure 6b); and an all-malic acid case with (5) 24% malic acid, 6% insoluble organics, and 70% inorganic salts (dotted line) and an all-citric acid case with (6) 24% citric acid, 6% insoluble organics, and 70% inorganic salts (dashed line) (Figure 6c).

ing to the bounding scenarios investigated here. These results suggest that these additional interactions have a negligible impact on hygroscopic growth (unless their organic interactions are significantly stronger than the model Na^+ and Cl^- ions), although major distinctions will occur in the deliquescence region.

5.3. Sensitivity to Estimated Organic Composition

The limited availability of data on the behavior of soluble and slightly soluble organic components has resulted in the simplified description of those components given in Table 2. While we cannot study the possible role of specific species whose thermodynamic behavior has not been characterized, we can compare the behavior of the components for which we do have data. In order to better illustrate differences from the base case behavior, we have omitted Mg^{2+} for this comparison.

The insoluble organic species are described as a detailed mixture of 20 species, but since they do not dissolve in the aqueous phase, their only role in particle properties is in how they contribute to the particle density and surface interactions. The surface properties will also rely heavily on individual particle morphologies. Figure 6a shows the difference between the estimated organic composition and a mixture of all-insoluble organic species. Removing the soluble organic species entirely reduces the hygroscopic growth by 10%.

The soluble species can also have very different influences on the hygroscopic growth, since the more soluble components deliquesce at lower relative humidities. In addition, the smaller organic ion species will take up more water on a mass basis. Figures 6b and 6c show the effect of replacing the mixture of soluble organic species with each of the four pure soluble components. A clear distinction appears below 70% relative humidity when fructose is removed, since no other species dissolves below 50%. In Figure 6b, at 70% the glucose dissolves and above 72% relative humidity the behavior of both the pure glucose and the pure fructose cases becomes indistinguishable from the base case organic mixture. Small differences can also be seen when malic acid or citric acid are considered in Fig. 6c, since neither dissolves before NaCl deliquesces.

5.4. Sensitivity to Empirical Correlations

All of the chemical activities and interfacial energies in equation (9) for pure components and their mixtures are derived from measurements in which experimental uncertainties are inherent. Since such errors can propagate in a calculation as complex as the one described here, we have varied individual empirical parameters in order to quantify the aggregate uncertainty in the model. While this calculation does not span the entire range of parameter space, it provides appropriate bounds on the uncertainties and some idea of the critical measurements required to improve model accuracy.

Table 4. Sensitivity of Model Predictions to Experimental Uncertainty in Data Used to Correlate Empirical Parameters

Interaction Parameters Between Functional Groups	Reference	Uncertainty of Experimental Measurements	Sensitivity of Predicted RH	
			at 73%	at 84%
CH_n and H_2O in multifunctional compounds	*Mertl* [1972]	±0.1% (mole fraction)	±1.0%	±0.6%
Sugars and H_2O	*Peres and Macedo* [1997]	±0.44%(RH)	±3.4%	±1.0%
Acids and H_2O	*Velezmoro et al.* [1998]	±0.15%(RH)	±2.9%	±1.0%
Acids and H_2O	*Apelblat et al.* [1995]	±14%(RH)	±1.6%	±1.1%
Sugars and ions	*Comesana et al.* [1999]	±0.5%(RH)	±3.1%	±1.0%
Acids and ions	*Herz and Hiebenthal* [1929]	±20%(mol L^{-1})	±4.2%	±1.4%

The experimental data are correlated in the model to estimate interaction parameters for each of the types of compounds described in the model. The five types of interactions needed to describe organic mixtures in sea salt are (1) interactions between multifunctional groups and water, (2) interactions between sugars and water, (3) interactions between carboxylic acids and water, (4) interactions between sugars and electrolytes, and (5) interactions between carboxylic acids and electrolytes. Table 4 summarizes these sensitivity studies: each sensitivity test was conducted by running the model with the extreme high and low values of the reported experimental data in the references given. Since the model is more sensitive at humidities near the deliquescence point, each calculation has been done at both a low relative humidity near deliquescence (73%) and a higher relative humidity (84%). The resulting changes in predicted hygroscopic growth are described by the percentage change in relative humidity. The estimated experimental uncertainties are within 5% change in the predicted equilibrium relative humidity. The so-called "salting out" effect between carboxylic acids and electrolytes can change the fraction of ions dissolved by up to 20%, resulting in up to a 4.2% difference in the equilibrium relative humidity at 73% relative humidity or up to a 1.6% difference at 84% relative humidity.

6. Conclusions

For the seawater organic species studied here, the presence of only 30% organic species in atmospheric particles at relative humidities higher than 50% reduces the predicted hygroscopic growth for an equilibrium internal mixture by 15% from the growth predicted for purely inorganic sea salt. Organic mass fractions of 50% or higher reduce growth by 25% compared to inorganic sea salt or eliminate water uptake entirely in subsaturated conditions. This effect may have important implications for particle behavior used for calculating global aerosol optical depths, since the magnitude is comparable to the inorganic composition differences studied by *Adams et al.* [1999]. Comparison to ambient hygroscopic growth factor measurements suggests that organic fractions of 10% to 30% are consistent with measured hygroscopic growth of ambient particles.

Significant uncertainties remain in the identification of the exact speciated composition of organic particles of marine origin. In addition, the behavior of the majority of existing organic species are not well characterized in complex mixtures with electrolytes in water. The sensitivity studies suggest that while the magnitude of the effect will vary with the exact speciated composition, the largest uncertainty lies in identifying the fraction of organic mass in the particle and the proportion of that organic mass that is soluble, slightly soluble, or insoluble.

Acknowledgments. This analysis was supported under Office of Naval Research grant N00014-97-1-0673. The authors are also grateful to Simon Clegg, John Prausnitz, Stanley Sandler, and their research groups for providing helpful insights for this work.

References

Abrams, D.S., and J.M. Prausnitz, Statistical thermodynamics of liquid mixtures: A new expression for the excess Gibbs energy of partly or completely miscible systems, *AIChE J., 21,* 116-128, 1975.

Adams, P.J., J.H. Seinfeld, and D.M. Koch, Global concentrations of tropospheric sulfate, nitrate, and ammonium aerosol simulated in a general circulation model, *J. Geophys. Res., 104,* 13,791-13,823, 1999.

Adamson, A.W., *Physical Chemistry of Surfaces*, John Wiley, New York, 1990.

Aluwihare, L.I., D.J. Repeta, and R.F. Chen, A major biopolymeric component to dissolved organic carbon in surface seawater, *Nature, 387,* 166-169, 1997.

Andrews, E., and S.M. Larson, Effect of surfactant layers on the size changes of aerosol-particles as a function of relative-humidity, *Environ. Sci. Technol., 27,* 857-865, 1993.

Apelblat, A., M. Dov, J. Wisniak, and J. Zabicky, The vapour pressure of water over saturated aqueous solutions of malic, tartaric, and citric acids, at temperatures from 288 K to 323 K, *J. Chem. Thermodyn., 27,* 35-41, 1995.

Benner, R., J.D. Pakulski, M. McCarthy, J.I. Hedges, and P.G. Hatcher, Bulk chemical characteristics of dissolved organic-matter in the ocean, *Science, 255,* 1561-1564, 1992.

Berg, O.H., E. Swietlicki, and R. Krejci, Hygroscopic growth of aerosol particles in the marine boundary layer over the Pacific and Southern Oceans during the First Aerosol Characterization Experiment (ACE 1), *J. Geophys. Res., 103,* 16,535-16,545, 1998.

Blanchard, D.C., Sea-to-air transport of surface active material, *Science, 146,* 396-397, 1964.

Blanchard, D.C., The production, distribution, and bacterial enrichment of sea-salt aerosol, in *Air-Sea Exchange of Gases and Particles*, pp. 407-454, D. Reidel, Norwell, Mass., 1983.

Clegg, S.L., K.S. Pitzer, and P. Brimblecombe, Thermodynamics of multicomponent, miscible, ionic-solutions, 2, mixtures including unsymmetrical electrolytes, *J. Phys. Chem., 96,* 9470-9479, 1992. (Correction, *J. Phys. Chem., 98,* 1368, 1994, and Correction, *J. Phys. Chem., 99,* 6755, 1995.)

Clegg, S.L., P. Brimblecombe, and A.S. Wexler, Thermodynamic model of the system H^+-NH_4^+-SO_4^{2-}-NO_3^--H_2O at tropospheric temperatures, *J. Phys. Chem. A, 102,* 2137-2154, 1998.

Clegg, S.L., J.H. Seinfeld, and P. Brimblecombe, Thermodynamic modelling of aqueous aerosols containing electrolytes and dissolved organic compounds, *J. Aerosol Sci., 32,* 713-738, 2001.

Comesana, J.F., A. Correa, and K. Sereno, Measurements of water activity in "sugar" plus sodium chloride plus water systems at 25°C, *J. Chem. Eng. Data, 44,* 1132-1134, 1999.

Creac'h, P.V., Presence of citric and malic acids in littoral marine waters, *Hebd. Seances Acad. Sci., 240,* 2551-2553, 1955.

Cruz, C.N., and S.N. Pandis, Deliquesence and hygroscopic growth of mixed inorganic-organic atmospheric aerosol, *Environ. Sci. Technol., 34,* 4313-4319, 2000.

Duce, R.A., V.A. Mohnen, P.R. Zimmerman, D. Grosjean, W. Cautreels, R. Chatfield, R. Jaenicke, J.A. Ogren, E. D. Pellizzari, and G.T. Wallace, Organic material in the global troposphere, *Rev. Geophys., 21,* 921-952, 1983.

Foster, M., and G.E. Ewing, An infrared spectroscopic study of water thin films on NaCl (100), *Surf. Sci., 428*, 102-106, 1999.

Foster, M.C., and G.E. Ewing, Adsorption of water on the NaCl(001) surface. II. An infrared study at ambient temperatures, *J. Chem. Phys., 112*, 6817-6826, 2000.

Fredenslund, A., J. Gmehling, and P. Rasmussen, *Vapor-Liquid Equilibrium Using UNIFAC,* Elsevier Sci., New York, 1977.

Freier, R.K., *Aqueous Solutions: Data for Inorganic and Organic Compounds*, W. de Gruyter, New York, 1976.

Gagosian, R.B., E.T. Peltzer, and O.C. Zafiriou, Atmospheric transport of continentally derived lipids to the tropical North Pacific, *Nature, 291,* 312-315, 1981.

Girshick, S.L., and C.-P. Chiu, Kinetic nucleation theory: A new expression for the rate of homogeneous nucleation from an ideal supersaturated vapor, *J. Chem. Phys., 93,* 1273-1277, 1990.

Gmehling, J., From UNIFAC to modified UNIFAC to PSRK with the help of DDB, *Fluid Phase Equilibr., 107,* 1-29, 1995.

Gmehling J., P. Rasmussen, and A. Fredenslund, Vapor-liquid equilibria by UNIFAC group contribution: Revision and extension, 2, *Ind. Eng. Chem. Process Des. Dev., 21,* 118-127, 1982.

Gogou, A.I., M. Apostolaki, and E.G. Stephanou, Determination of organic molecular markers in marine aerosols and sediments: One-step flash chromatography compound class fractionation and capillary gas chromatographic analysis, *J. Chromatogr. A, 799,* 215-231, 1998.

Hämeri, K., M. Väkevä, H.C. Hansson, and A. Laaksonen, Hygroscopic growth of ultrafine ammonium sulfate aerosol measured using a ultrafine tandem differential mobility analyzer, *J. Geophys. Res., 105,* 22,231-22,242, 2000.

Hansson, H.C., M.J. Rood, S. Koloutsou-Vakakis, K. Hämeri, D. Orsini, and A. Wiedensohler, NaCl aerosol particle hygroscopicity dependence on mixing with organic compounds, *J. Atmos. Chem., 31,* 321-346, 1998.

Haywood, J.M., and V. Ramaswamy, Global sensitivity studies of the direct radiative forcing due to anthropogenic sulfate and black carbon aerosols, *J. Geophys. Res., 103,* 6043-6058, 1998.

Haywood, J.M., V. Ramaswamy, and B.J.Soden, Tropospheric aerosol climate forcing in clear-sky satellite observations over the oceans, *Science, 283,* 1299-1303, 1999.

Herz, W., and F. Hiebenthal, Über Löslichkeitsbeeinflussungen, *Z. Anorg. Allg. Chem., 177,* 363-380, 1929.

Hoffman, E.J., and R.A. Duce, Factors influencing the organic carbon content of marine aerosol: A laboratory study, *J. Geophys. Res., 81,* 3667-3670, 1976.

Israelachvili, J.N., *Intermolecular and Surface Forces,* Academic, San Diego, Calif., 1996.

Kawamura, K., and R.B. Gagosian, Midchain ketocarboxylic acids in the remote marine atmosphere: Distribution patterns and possible formation mechanisms, *J. Atmos. Chem., 11,* 107-122, 1990.

Kawamura K, R. Semere, Y. Imai, Y. Fujii, and M. Hayashi, Water soluble dicarboxylic acids and related compounds in Antarctic aerosols, *J. Geophys. Res., 101,* 18,721-18,728, 1996.

Kojima, K., S.J. Zhang, and T. Hiaki, Measuring methods of infinite dilution activity coefficients and a database for systems including water, *Fluid Phase Equilibr., 131,* 145-179, 1997.

Li, J.D., H.M. Polka, and J. Gmehling, A G(E) model for single and mixed-solvent electrolyte system, 1, Model and results for strong electrolytes, *Fluid Phase Equilibr., 94,* 89-114, 1994.

Li, Z.B., Y.G. Li, and J.F. Lu, Surface tension model for concentrated electrolyte aqueous solutions by the Pitzer equation, *Ind. Eng. Chem. Res., 38,* 1133-1139, 1999.

Li, Z.D., A.L. Williams, and M.J. Rood, Influence of soluble surfactant properties on the activation of aerosol particles containing inorganic solute, *J. Atmos. Sci., 55,* 1859-1866, 1998.

Lyman, W.J., W.F. Reehl, and D.H. Rosenblatt, *Handbook of Chemical Property Estimation Methods: Environmental Behavior of Organic Compounds*, Am. Chem. Soc., Washington, D.C., 1990.

Menzel, D.W., and J.H. Ryther, Distribution and cycling of organic matter in the oceans, in *Symposium on Organic Matter in Natural Waters*, edited by D. W. Hood, Inst. of Mar. Sci., pp. 31-54, Univ. of Alaska, Fairbanks, 1970.

Mertl, I., Liquid-vapor equilibrium 50. Prediction of multicomponent vapor-liquid equilibria from binary parameters in systems with limited miscibility, *Collect. Czech. Chem. Commun., 37,* 375-411, 1972.

Michalewicz, Z., and G. Nazhiyath, Genocop III: A coevolutionary algorithm for numerical optimization problems with nonlinear constraints, in *Proc. 2nd IEEE International Conference on Evolutionary Computation, Perth, 2,* pp. 647-651, Inst. of Electr. and Electr. Eng., New York, 1995.

Middlebrook, A.M., D.M. Murphy, and D.S. Thomson, Observations of organic material in individual marine particles at Cape Grim during the First Aerosol Characterization Experiment (ACE 1), *J. Geophys. Res., 103,* 16,475-16,483, 1998.

Mirabel, P., H. Reiss, and R.K. Bowles, A theory for the deliquescence of small particles, *J. Chem. Phys., 113,* 8200-8205, 2000.

Nath, S., Surface tension of nonideal binary liquid mixtures as a function of composition, *J. Colloid Interface Sci., 209,* 116-122, 1999.

Peres, A.M., and E.A. Macedo, A modified UNIFAC model for the calculation of thermodynamic properties of aqueous and non-aqueous solutions containing sugars, *Fluid Phase Equilibr., 139,* 47-74, 1997.

Peters, S.J., and G.E. Ewing, Thin film water on NaCl(100) under ambient conditions: An infrared study, *Langmuir, 13,* 6345-6348, 1997a.

Peters, S.J., and G.E. Ewing, Water on salt: An infrared study of adsorbed H2O on NaCl(100) under ambient conditions, *J. Phys. Chem. B, 101,* 10,880-10,886, 1997b.

Peters, C.A., K.H. Wammer, and C.D. Knightes, Multicomponent NAPL solidification thermodynamics, *Trans. Porous Med., 38,* 57-77, 2000.

Pitzer, K.S., Ion interaction approach: Theory and data, in *Activity Coefficients in Electrolyte Solutions,* edited by K. S. Pitzer, pp. 75-153, CRC Press, Boca Raton, Fla., 1991.

Pividal, K.A., and S.I. Sandler, Neighbor effects on the group contribution method–Infinite dilution activity-coefficients of binary-systems containing primary amines and alcohols, *J. Chem. Eng. Data, 35,* 53-60, 1990.

Quinn, J.A., R.A. Steinbrook, and J.L. Anderson, Breaking bubbles and the water-to-air transport of particulate matter, *Chem. Eng. Sci., 30,* 1177-1184, 1975.

Quinn, P.K., D.J. Coffman, V.N. Kapustin, T.S. Bates, and D.S. Covert, Aerosol optical properties in the marine boundary layer during the First Aerosol Characterization Experiment (ACE 1) and the underlying chemical and physical aerosol properties, *J. Geophys. Res., 103,* 16,547-16,564, 1998.

Quinn, P.K., T.S. Bates, D.J. Coffman, T.L. Miller, J.E. Johnson, D.S. Covert, J.-P. Putaud, C. Neusüss, and T. Novakov, A comparison of aerosol chemical and optical properties from the 1st and 2nd Aerosol Characterization Experiments, *Tellus, Ser. B, 52,* 239-257, 2000.

Reid, R.C., J.M. Prausnitz, and B.E. Poling, *The Properties of Gases and Liquids,* McGraw-Hill, New York, 1987.

Riley, J.P., and R. Chester, *Introduction to Marine Chemistry,* Academic, San Diego, Calif., 1971.

Riley, J.P., and D. Segar, Seasonal variation of the free and combined dissolved amino acids in the Irish Sea, *J. Mar. Biol. Assoc. U. K., 50,* 713-720, 1970.

Rogge, W.F., M.A. Mazurek, L.M. Hildemann, G.R. Cass, and B.R.T. Simoneit, Quantification of urban organic aerosols at a molecular level: Identification, abundance and seasonal variation, *Atmos. Environ., Part A, 27,* 1309-1330, 1993.

Russell, L.M., and Y. Ming, Deliquescence of small particles, *J. Chem. Phys.,* in press, 2001

Saxena, P., and L.M. Hildemann, Water-soluble organics in atmospheric particles: A critical review of the literature and application of thermodynamics to identify candidate compounds, *J. Atmos. Chem., 24,* 57-109, 1996.

Saxena, P., and L.M. Hildemann, Water absorption by organics: Survey of laboratory evidence and evaluation of UNIFAC for estimating water activity, *Environ. Sci. Technol., 31,* 3318-3324, 1997.

Seinfeld, J.H., and S.N. Pandis, *Atmoshpeirc Chemistry and Physics,* John Wiley, New York, 1997.

Stokes, R.H., and R.A. Robinson, Interactions in aqueous nonelectrolyte solutions, I, Solute-solvent equilibria, *J. Phys. Chem., 70,* 2126-2130, 1966.

Swietlicki, E., et al., Hygroscopic properties of aerosol particles in the northeastern Atlantic during ACE-2, *Tellus, Ser. B, 52,* 750-778, 2000.

Tang, I.N., and H.R. Munkelwitz, Aerosol phase transformation and growth in the atmosphere, *J. Appl. Meteorol., 33,* 792-796, 1994.

Tang, I.N., A.C. Tridico, and K.H. Fung, Thermodynamic and optical properties of sea salt aerosols, *J. Geophys. Res., 102,* 23,269-23,275, 1997.

Turpin, B.J., and H.J. Lim, Species contributions to PM2.5 mass concentrations: Revisiting common assumptions for estimating organic mass, *Aerosol Sci. Technol., 35,* 602-610, 2001.

Velezmoro, C.E., and A.J.A. Meirelles, Water activity in solutions containing organic acids, *Dry Technol., 16,* 1789-1805, 1998.

Weis, D.D., and G.E. Ewing, Infrared spectroscopic signatures of $(NH_4)_2SO4$ aerosols, *J. Geophys. Res., 101,* 18,709-18,720, 1996.

Wilemski, G., The Kelvin equation and self-consistent nucleation theory, *J. Chem. Phys., 103,* 1119-1126, 1995.

Wu, H.S., and S.I. Sandler, Proximity effects on the predictions of the UNIFAC model, 1, ethers, *AIChE J., 35,* 168-172, 1989.

Wu, H.S., and S.I. Sandler, Use of ab initio-quantum mechanics calculations in group contribution methods, 2, Test of new groups in UNIFAC, *Ind. Eng. Chem. Res., 30,* 889-897, 1991.

Xie, W.H., W.Y. Shiu, and D. Mackay, A review of the effect of salts on the solubility of organic compounds in seawater, *Mar. Environ. Res., 44,* 429-444, 1997.

Zhang, Y., C. Seigneur, J.H. Seinfeld, M. Jacobson, S.L. Clegg, and F.S. Binkowski, A comparative review of inorganic aerosol thermodynamic equilibrium modules: Similarities, differences, and their likely causes, *Atmos. Environ., 34,* 117-137, 2000.

Zhou, J., E. Swietlicki, O.H. Berg, P.P. Aalto, K. Hämeri, E.D. Nilsson, and C. Leck, Hygroscopic properties of aerosol particles over the central Arctic Ocean during summer, *J. Geophys. Res.,* in press, 2001.

L.M. Russell, Department of Chemical Engineering, A317 Engineering Quadrangle, Princeton University, Princeton, NJ 08544, USA. (lrussell@princeton.edu)

Y. Ming, Department of Civil and Environmental Engineering, A316 Engineering Quadrangle, Princeton University, Princeton, NJ 08544, USA. (mingyi@Princeton.edu)

(Received January 17, 2001; revised July 15, 2001; accepted July 17 , 2001.)